

High-Speed Imaging Diagnostics Applied to the Study of Auto-Ignition of Methane Jets in a Hot Coflow

W. Meier¹, C.M. Arndt¹, J. Gounder¹, I. Boxx¹, K. Marr²,

¹Institut für Verbrennungstechnik, Deutsches Zentrum für Luft- und Raumfahrt (DLR)
Stuttgart, Germany

²Department of Aerospace Engineering & Engineering Mechanics,
University of Texas at Austin
Austin, Texas, USA

1 Introduction

Auto-ignition of fuel in hot oxidizing gas is of importance for various technical applications, for example in internal combustion engines, scramjets, or gas turbine combustors. The physical and chemical processes involved in auto-ignition are very complex and highly sensitive to boundary conditions like temperature, pressure, gas composition, residence time and turbulence level [1], and a detailed understanding of the processes is subject of current research activities. Except for very simple configurations, the experimental investigation of auto-ignition is quite challenging due to the instationarity and short time scales involved. Here, innovative high-speed lasers and cameras afford the opportunity to resolve the temporal development of an ignition and flame kernel development process [2-4]. However, the spatial resolution is often limited, either due to the line-of-sight integration of chemiluminescence imaging or, for laser light sheet measurements, by the missing information from outside the laser sheet.

An experimental concept that has been used recently in various configurations to study auto-ignition and flame stabilization is the injection of a turbulent fuel jet into a hot coflow [5-9]. It was concluded from those investigations that the stabilization of the lifted jet flame is caused by auto-ignition rather than turbulent flame propagation. In the investigations reported here, a pulsed methane jet was injected into the exhaust gas of a flat, lean premixed H₂/air flame. The measurements captured the beginning of the injection, the jet development, the auto-ignition events, the flame kernel development and finally the stably burning lifted flame. Several high-speed imaging techniques were applied at 5 or 10 kHz repetition rate: OH* chemiluminescence and broadband luminescence imaging, Schlieren imaging and planar laser induced fluorescence (PLIF) of OH. To achieve better spatial resolution OH PLIF images were recorded simultaneously with luminescence images at a different angle of detection. In this way it was possible to distinguish between ignition events which took place within the laser sheet and those flame kernels which propagated into the laser sheet.

The time and downstream positions of first auto-ignition events after injection were identified in many runs at identical operating conditions. This position was compared with the downstream position where the stably burning lifted flame was stabilized. These positions were close to each other,

however, the stabilization region of the flame fluctuated due to auto-ignition events close to the lift-off height.

2 Experiment

The burner is shown schematically in Fig.1. A lean premixed flat laminar H_2 /air flame was stabilized on a water-cooled sintered bronze matrix of $75 \times 75 \text{ mm}^2$ cross section. A stainless steel tube (i.d. 2 mm, o.d. 3 mm) for fuel injection was inserted along the burner axis and stucked 8 mm out of the burner matrix. Compared to a previous setup [9], the tube is much smaller and not water-cooled so that heat loss of the flame at the fuel tube is negligible. A pulsed solenoid valve (2/2-way Spider valve) was installed at the lower end of the tube to enable a pulsed injection. The burner was confined by 4 quartz plates held by posts in the corners to prevent entrainment of room air and to enable optical access. The operating conditions of the H_2 /air flame were chosen in such a way that auto-ignition occurred a few centimeters downstream. The exhaust gas composition was deduced from the flow rates using an equilibrium calculation [10] and the temperatures were taken from measurements with coherent anti-Stokes Raman scattering in a similar burner [11]. The flow rates of the H_2 /air mixtures used were high enough that heat transfer from the flame to the bronze matrix was negligible. Thus, the flames reached nearly adiabatic flame temperature [11]. Taking uncertainties of the flow rates on the order of 1 - 1.5% into account, the accuracy of the temperature is estimated to be around 2%.

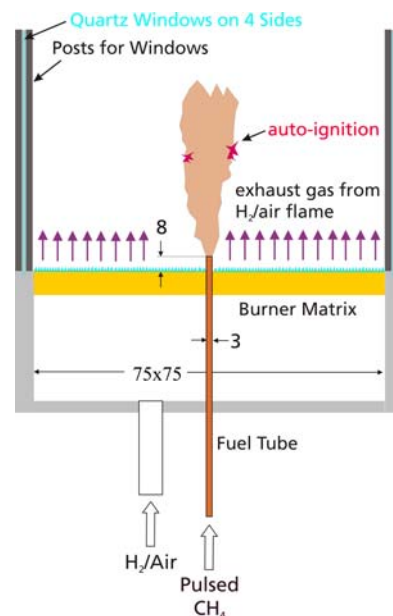


Figure 1: Schematic of the burner.

For the results presented in this paper, the following operating conditions were applied. The H_2 and air flow rates of the flat flame were 42.4 slpm and 208.8 slpm, respectively, corresponding to an equivalence ratio of 0.485 and an adiabatic flame temperature of 1613 K. The mean flow velocity of the exhaust gas, calculated from the flow rates for $T=1613 \text{ K}$ was 4.03 m/s. The calculated exhaust gas equilibrium composition was 71.69% N_2 , 18.47% H_2O , 9.81% O_2 and 0.023% OH . At steady state conditions, the CH_4 jet had an exit velocity of about 100 m/s corresponding to a Reynolds number of approximately 13000. The exact temporal development of the jet exit velocity after opening the valve is not known, however, the measurements yield some information about it. A steady lift-off height of the flame was reached a few milliseconds after the first auto-ignition event. The upper 6-8 mm of the fuel tube which were exposed to the flame, became relatively hot. The rest of the tube was at room temperature because the matrix was water-cooled.

The chemiluminescence was recorded by two highspeed CMOS cameras (LaVision HSS5 and HSS6). The HSS5 was equipped with an image intensifier (LaVision HS-IRO) and a bandpass interference filter with high transmission around 310 nm for the detection of OH chemiluminescence (termed OH^*). The exposure time was 25 μs . The second camera was operated without intensifier and filter and captured the broadband luminescence in a spectral range from approximately 350 to 1000 nm with an exposure time of 200 μs . Chemiluminescence is emitted by species which are formed in excited electronic states in the flame reactions, for example OH , CH , C_2 or CO_2 [12]. Because the lifetime in the excited state is on the order of nanoseconds at atmospheric pressure, the chemiluminescence reflects the location of combustion activity. In the red and near infrared spectral region thermally excited water molecules can also contribute to the flame luminosity, however, this emission is not generated by chemical reactions [13]. In contrast to electronically excited OH^* , OH in the electronic ground state is present in the reaction zone as well as in hot burned gas. For its detection planar laser-induced fluorescence (PLIF) was applied. The OH PLIF system consisted of a frequency doubled dye laser and an intensified CMOS camera. The dye laser (Sirah Cobra-Stretch HRR, using

Rhodamine 6G, $\lambda \approx 566$ nm) was pumped with a frequency doubled, diode-pumped solid state Nd:YLF laser (Edgewave IS-8III, 8 ns pulse duration) at 5 kHz repetition rate. After frequency doubling, the output was 0.1 mJ/pulse at 283.2 nm. The wavelength was tuned to the peak of the $Q_1(7)$ line of the A-X ($v'=1$, $v''=0$) transition of OH. The beam was formed into a sheet of ≈ 40 mm height in the combustion chamber and focused to a waist of ≈ 0.4 mm. The fluorescence was detected at 90° through a bandpass interference filter by an intensified CMOS camera (LaVision HS-IRO, LaVision HSS5) equipped with a UV achromatic lens (Cerco, $f=45$ mm).

The z co-ordinate is defined as the flow direction, x is in direction of the laser beam and y is perpendicular to the laser sheet. The intensified cameras for the detection of PLIF and OH* chemiluminescence were arranged in y -direction at opposite sides of the burner. The non-intensified CMOS camera for the detection of broadband chemiluminescence was setup in x -direction slightly above the laser sheet and inclined with respect to the laser beam to image the flame area of interest. The trigger pulses for the valve, the laser and the cameras were supplied by a timing unit.

3 Results and Discussion

The procedure of the measurements was as follows. The lean H_2 /air flame was operated for about 15 minutes in order to reach thermal equilibrium of the burner before the injection of the pulsed CH_4 jet was initiated. The laser was running continuously. A trigger pulse was sent to simultaneously initiate the opening of the valve and begin a fixed-length image acquisition sequence by the high-speed cameras. The OH* and broadband chemiluminescence cameras were triggered simultaneously, 1 μ s after the OH PLIF camera.

Figure 2 shows a sequence of single-shot exposures from one measurement run. In the first two rows, OH PLIF images are displayed which cover a downstream distance from $z=15$ to 55 mm. The time displayed at the top of each image is the elapsed time after the trigger pulse for the valve (the valve did not open immediately with the trigger pulse but roughly with 3.2 ms delay). The OH PLIF image at $t=4$ ms shows an evenly distributed low signal level with an OH-free region around $x=0$ and up to $z \approx 40$ mm. The low OH PLIF signal reflects the hot coflow from the premixed H_2 /air flame and the OH-free region the CH_4 jet. The OH from the coflow is expected to disappear rapidly as soon as CH_4 is mixed into the exhaust gas due to the temperature drop and OH depletion by chemical reactions. The diameter of the jet deduced from this image is approximately 8 mm. In the next image at $t=4.2$ ms the tip of the jet has reached to $z \approx 50$ mm. In the following 0.6 ms the leading edge of the jet has moved out of the field of view and in the imaged section, more wrinkles have developed. At 5 ms bright spots appear at $z \approx 18$ mm on the left side and $z \approx 35$ mm on the right side indicating the presence of flame kernels. While the flame kernel on the left side exhibits hardly any growth, the one on the right side becomes larger and moves slowly downstream. Later more flame islands appear which finally develop to a stably burning lifted flame.

It must be kept in mind, that the imaged OH distributions are limited to the plane of the laser sheet and do not reflect the development in 3 dimensions. The line-of-sight integrated OH* imaging (acquired simultaneously by the camera at the opposite side of the combustion chamber) provides further spatial information on flame kernel development. The OH* images corresponding to $t = 4.8 - 5.4$ ms are shown in the third row of Fig. 2. In this sequence several spots of high OH* emission are seen at 5 ms which grow rapidly in size and intensity and finally merge to one large flame region, at least in the line-of-sight integrated images. The images of the fourth row display the line-of-sight integrated visible flame luminosity observed in x -direction. The non-intensified camera used on this side has a lower sensitivity and the weak emission at 5 ms might have been below the detection limit or there was no broadband luminosity in the early stage of flame kernel development. However, at 5.2 ms two flame kernels are observed which, again, are seen to grow in size and intensity. From the image at 5.2 ms it is inferred that the first appearance of the more intense ignition kernel is within or at least very close to the laser sheet. Thus, in this image series, the OH PLIF measurement captured the beginning of the auto-ignition event and the observed development of structure and intensity are representative of auto-ignition and not of an established flame propagating into the light sheet. The OH PLIF technique

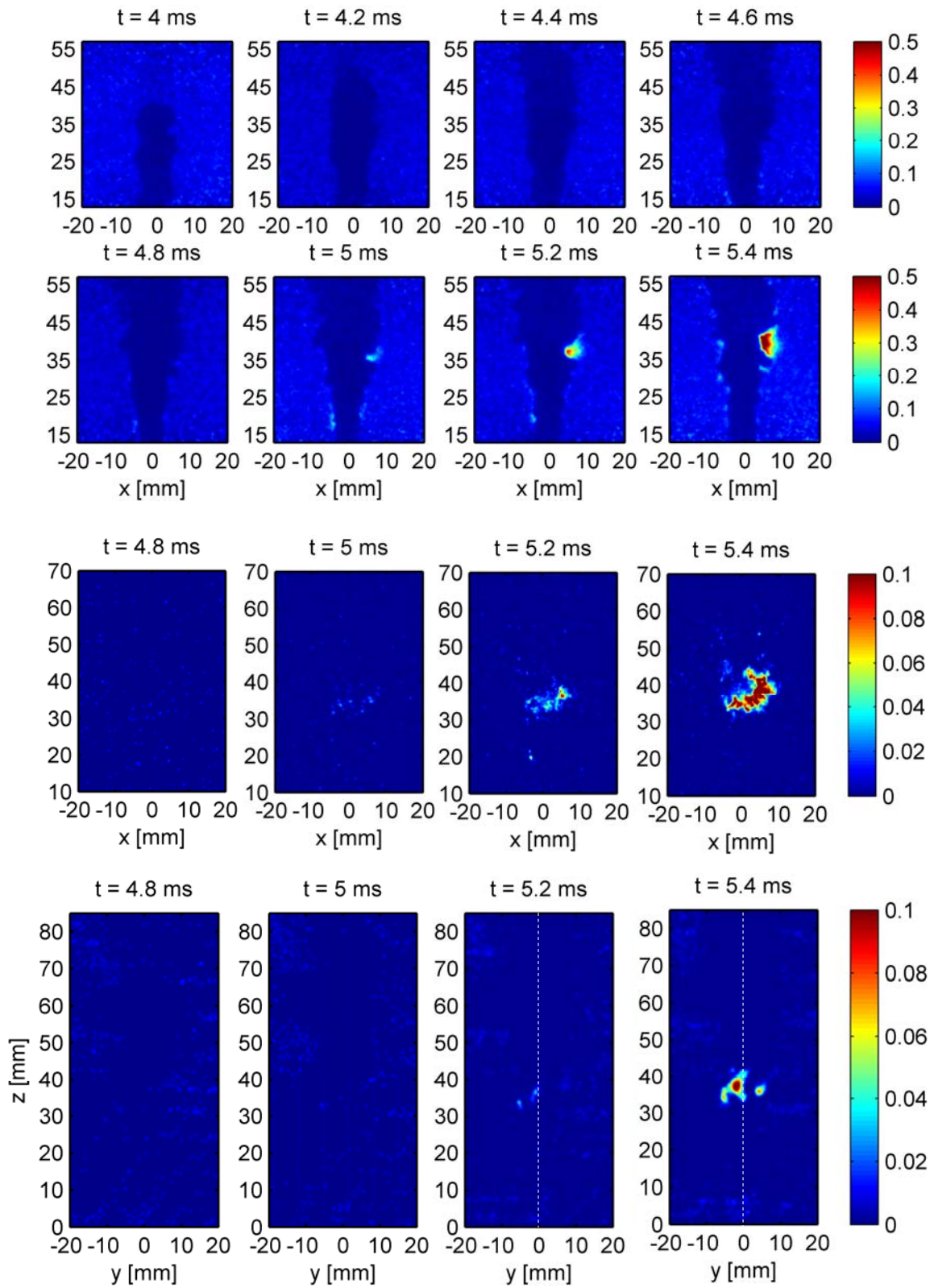


Figure 2: Simultaneously recorded sequences from high-speed imaging. First 2 rows: OH PLIF; third row: OH* chemiluminescence; fourth row: broadband chemiluminescence detected at 90° with respect to the other images. The dashed line in the last images indicate the position of the laser sheet for OH LIF excitation.

yields a higher sensitivity and better spatial and temporal resolution than chemiluminescence imaging. The chemiluminescence images, on the other hand, yield additional information about the spatial structures and particularly the position of the flame kernel with respect to the light sheet. In this way, the combined high-speed imaging techniques enable a detailed characterization of the ignition process. The evaluation of 160 measurement series at identical experimental conditions revealed that auto-ignition always occurred at the periphery of the jet. The average downstream location of the first ignition spot was $z=32.9$ mm with an RMS of 5.3 mm. Often ignition occurred almost simultaneously at different locations. The expansion of the flame kernels was significantly faster than the downstream convection. The velocity of the downstream convection was difficult to determine accurately because it was overlaid by the growth of the flame kernel. However, an estimation resulted in a speed of roughly 5 m/s. It is not surprising that this value is close to the coflow velocity because the stoichiometric mixture fraction is $f_{\text{stoich.}}=0.029$ and the most reactive mixture fraction is expected to be even smaller than $f_{\text{stoich.}}$ [1]. If, for a rough estimation, conservation of the axial momentum of the jet and co-flow fluid within the mixture is assumed, the axial velocity of the most reactive mixtures should be very close to the co-flow velocity, i.e. these mixtures are located at the periphery of the jet. Figure 3 presents instantaneous distributions of OH PLIF, OH* and broadband luminescence from the stably burning lifted flame at steady state conditions. The images show that the flame fronts are corrugated and not homogeneously distributed. However, the focus of this study is not on the shape of the lifted flame but on the stabilization region. The lift-off height deduced from the OH* images is $z\approx 35$ mm and lies very close to the downstream position where the first auto-ignition occurred, $z\approx 32.9$ mm. This finding supports the explanation that the flame is stabilized by auto-ignition. However, it was difficult to define the lift-off height exactly because the flame anchoring location fluctuated by some millimeters. Often, auto-ignited flame islands appeared from as far as $z\approx 24$ mm below and moved downstream to merge with the main flame. The influence of the coflow temperature on the relationship between lift-off height and location of first appearance of auto-ignition is subject of the further data evaluation.

In conclusion, the presented experimental setup enabled the time and spatially resolved investigation of auto-ignition of a pulsed methane jet in a vitiated coflow. Auto-ignition kernels appeared quite reproducible at the periphery of the jet and expanded rapidly. The stabilization region of the steady burning lifted flame was very close to the downstream position of first auto-ignition.

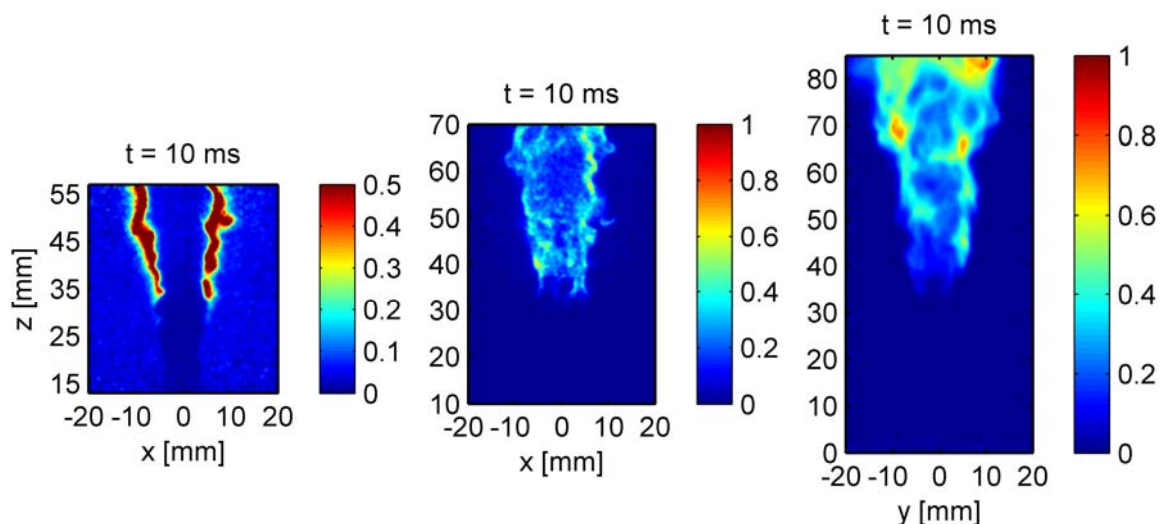


Figure 3: Stably burning lifted flame recorded at 10 ms. Left: OH PLIF; middle: OH* chemiluminescence; right: broadband luminescence at 90° with respect to the other images.

References

- [1] Mastorakos E. (2009). Ignition of Turbulent Non-Premixed Flames, *Prog. Energy Combust. Sci.* 35: 57
- [2] Fajardo C, Sick V. (2009). Development of a High-Speed UV Particle Image Velocimetry Technique and Application for Measurements in Internal Combustion Engines. *Exp. Fluids* 46: 43.
- [3] Kittler C, Böhm B, Ahmed SF, Gordon R, Boxx I, Meier W, Dreizler A, Mastorakos E. (2009). Statistics of Relative and Absolute Velocities of Turbulent Non-Premixed Edge Flames Following Spark Ignition. *Proc. Combust. Inst.* 32: 2957.
- [4] Mosbach T, Sadanandan R, Meier W, Eggels R. (2010). Experimental Analysis of Altitude Relight under Realistic Conditions using Laser and High-Speed Video Techniques. *Proc. ASME Turbo Expo, GT2010-22625*.
- [5] Cabra R, Chen JY, Dibble RW, Karpetis AN, Barlow RS. (2005). Lifted Methane-Air Jet Flame in a Vitiated Coflow. *Combust. Flame* 143: 491.
- [6] Gordon RL, Masri AR, Mastorakos E. (2008). Simultaneous Rayleigh Temperature, OH- and CH₂O-LIF Imaging of Methane Jets in a Vitiated Coflow. *Combust. Flame* 155: 181.
- [7] Medwell PR, Kalt PAM, Dally BB. (2008). Simultaneous imaging of OH, formaldehyde, and temperature of turbulent nonpremixed jet flames in a heated and diluted coflow. *Combust. Flame* 148: 48.
- [8] Oldenhof E, Tummers MJ, van Veen EH, Roekaerts DJEM. (2010). Ignition kernel formation and lift-off behaviour of jet-in-hot-coflow flames. *Combust. Flame* 157: 1167.
- [9] Meier W, Boxx I, Arndt C, Gamba M, Clemens N. (2011). Investigation of auto-ignition of a pulsed methane jet in vitiated air using high-speed imaging techniques. *J. Eng. Gas Turbines Power* 133: 021504.
- [10] Morley C. Gaseq, a chemical equilibrium program for windows, URL <http://gaseq.co.uk>.
- [11] Prucker S, Meier W, Stricker W. (1994). A Flat Flame Burner as Calibration Source for Combustion Research: Temperatures and Species Concentrations of Premixed H₂/Air Flames. *Rev. Sci. Instrum.* 65: 2908.
- [12] De Leo M, Saveliev A, Kennedy LA, Zelepouga SA. (2007). OH and CH luminescence in opposed flow methane oxy-flames. *Combust. Flame* 149: 435.
- [13] Schefer RW, Kulatilaka WD, Patterson BD, Settersten TB (2009). Visible emission of hydrogen flames. *Combust. Flame* 156: 1234.